Article:

Mutumba, A, Cheeseman, K, Clarke, H et al. (1 more author) (2018) Design and development of a direct injection system for cryogenic engines. Cryogenics, 91. pp. 77-86. ISSN 0011-2275

https://doi.org/10.1016/j.cryogenics.2017.12.009

Design and development of a direct injection system for cryogenic engines

Angela Mutumba[1], Kevin Cheeseman[2], Henry Clarke[2], Dongsheng Wen[1,3,*]

[1]School of Chemical and Process Engineering, University of Leeds, Leeds, LS2 9JT, U.K.

[2]Dearman Engine Company Ltd. London, UK

[3]School of Aeronautic Science and Engineering, Beihang University, Beijing, P.R.China

Abstract

The cryogenic engine has received increasing attention due to its promising potential as a zero-emission engine. In this study, a new robust liquid nitrogen injection system was commissioned and set up to perform high pressure injections into an open vessel. The system is used for quasi-steady flow tests used for the characterisation of the direct injection process for cryogenic engines. An electro-hydraulic valve actuator, provides intricate control of the valve lift, with a minimum cycle time of 3 milliseconds and a frequency of up to 20 Hz. With additional sub-cooling, liquid phase injections from 14 - 94 bar were achieved. Results showed an increase in the injected mass with the increase in pressure, and decrease in temperature. The injected mass was also observed to increases linearly with the valve lift. Better control of the injection process,

minimises the number of variables, providing more comparable and repeatable sets of data. Implications of the results on the engine performance were also discussed.

Keywords: Cryogenic engine injection, Liquid nitrogen, Hydraulic valve actuator, Thermal energy, Zero emission engine

1. Introduction

The cryogenic engine is a zero-emission combustion free engine designed to deliver power from cold. The engine uses a typical Rankine cycle with a near-isothermal expansion of liquid air or nitrogen from low grade/ ambient heat to convert heat energy into work[1]. With a limited engine power of ~0.2 kWh/kg of fuel (one ref here), the engine is aimed at providing auxiliary power and air conditioning for refrigeration hybrid heavy-duty vehicles. The performance and efficiency of the engine are solely based on the expansion, which is driven by the speed of the heat transfer process. Previous designs involved the indirect expansion of the cryogen using a heat exchanger, but were limited by its efficiency, and added to the overall bulk and mass of the design. More recently, the Dearman engine[2] was designed in order to achieve higher efficiencies using in-cylinder heat transfer, which is achieved by the direct injection of the cryogen into a heat transfer fluid (HEF). The heat transfer is enhanced by direct contact and increased interfacial area between the two fluids[3]. The process is entirely controlled by the injection and mixing of the cryogen in the cylinder.

High pressure cryogenic injection has been of great interest for power and propulsion systems in the aerospace industry. Although extensive experimental and numerical studies[4-7] have been conducted to characterize and understand the cryogenic flow dynamics involved in the injection and mixing process, only a few authors have attempted to investigate injections specific to reciprocating cryogenic engines[3, 8-12]. For example, Clarke et al.[3] demonstrated the benefits of the mass transfer, latent heat and sensible heat transfer of liquid nitrogen, as well as the use of water as the heat transfer fluid, which were influenced significantly by the injection parameters. Despite the linear correlation between the injection pressure and pressurisation rates, it was noted that the intake pressure would be limited by the onset of cavitation and chocking at a certain point. At this point, the flow velocity becomes non-responsive to the increase of the upstream or decrease of the downstream pressure. This critical point, based on the ratio of the downstream and upstream pressure, would determine the peak engine pressure under specific conditions. The onset of chocking occurs approximately 50 % lower than the critical pressure ratio[13]. The effects of chocking are not considered because the pressure at which this maximum is reached is above the injection pressures tested here. This work is an extension of the work done by Mohr et al.[14]investigating high pressure flow through a poppet valve for the Dearman engine but with the use of liquid nitrogen rather than gas.

Earlier work was limited to low injection pressure due to the experimental constraints. Additionally, closed cylinder injections meant that the mass flow during the injection cycle could not be measured, but only determine once the valve was closed. Therefore, the injected mass at any time during the injection cycle was unknown. Repeatability and comparison of the results was also an issue especially with the lack of information on valve timings and injection duration and therefore further testing is needed in this area.

The mass transfer into the engine is key expansion and pressurisation in the engine and therefore key to its overall performance. Precise control of the valve lift and speed is necessary to analyse and understand the mass transfer during the injection cycle. However, experiments in this area present several challenges due to the complexity of the injection process. For example, the adequate supply of the cryogen at sub-cooled temperatures (77-126 K) is difficult to maintain. Secondly, high pressure injections coupled with short valve timings are necessary to maximise the injected mass. The rapid valve movement is required to prevent backflow, as the cylinder-pressure approaches to that in the injection line. Consequently, a robust high speed valve actuation system capable of the task within a few milliseconds is also necessary for the experiments.

This paper describes the design and operation of a purposely built rig to conduct off engine tests for the high pressure injection of liquid nitrogen. With increased pressure, we expect higher flow velocities of the injected jet, which would enhance the mixing and ultimately, the heat transfer. The system is used for a quasi-steady flow characterisation of the LN_2 injector, as a vital stage of investigations into direct injection for cryogenic engines. An electro-hydraulic valve actuation (EHVA) system is used to control the movement of the poppet valve in the LN_2 injector. This valve actuation system is needed to allow for a rapid and timely valve movement. LN_2 is shot into an open vessel, in order measure the injected mass during the injection cycle. Pressure and temperature readings at the injector are used to determine the thermodynamic state of the nitrogen. The effect of injection parameters on the mass flow is discussed, as well as the implications for the engine performance.

2. Structure of injection system

2.1 Injector

The spray quality is highly dependent on the design of the injector and the injection pressure. The injector used is provided by Dearman Engine Company Ltd and is designed specifically for cryogenic injection. It is made of stainless steel because of high cryogenic toughness and consistent thermal expansion at the operating sub-zero temperatures. The injector consists of a poppet valve, which is attached to the head of the injector. The inlet and outlet lines are both angled, to reduce the pumping force at the inlet, whilst increasing it at the outlet. This prevents the cryogen from flowing out of injector too quickly. The inlet feedline is slightly extended to allow for a steady laminar flow before the valve is opened.

An ultra-high-molecular-weight-polyethylene (UHMWPE) seat is pressed onto the base of the poppet valve to reduce the wear resulting from impact during movement. The thermoplastic material is used for its low density; high impact strength; ductility; abrasion resistance; chemical resistance and self-lubricating properties[15, 16]. UHMWPE also has excellent sealing properties[17], which are vital to prevent any leakage when the valve is closed. UHMWPE and stainless steel were selected for their compatibility and low shrinkage percentage (less than 1%). At low temperatures, the hardness and friction coefficient of the plastic increases and it begins to display characteristics of fatigue and abrasive wear[18]. The increased hardness is attributed to the closely packed micro-structure at low temperatures, hindering the movement/slip of the molecular chains. The ductility of the material is lost, therefore reducing its ability to absorb energy during compressions. Although its fatigue life cycle at low temperatures is unclear, the seal did not demonstrate any sign of leakage and did not require replacement during the project period. Before testing, the valve was checked for leakage using both high pressure gas and liquid nitrogen.

The injector assembly also consists of a spring underneath the injector head. The movement of the poppet valve is controlled by the EHVA unit that is coupled (Figure 1) to the injector, where it applies a 4.2kN force transmitted through the springs. (Insert Figure1)

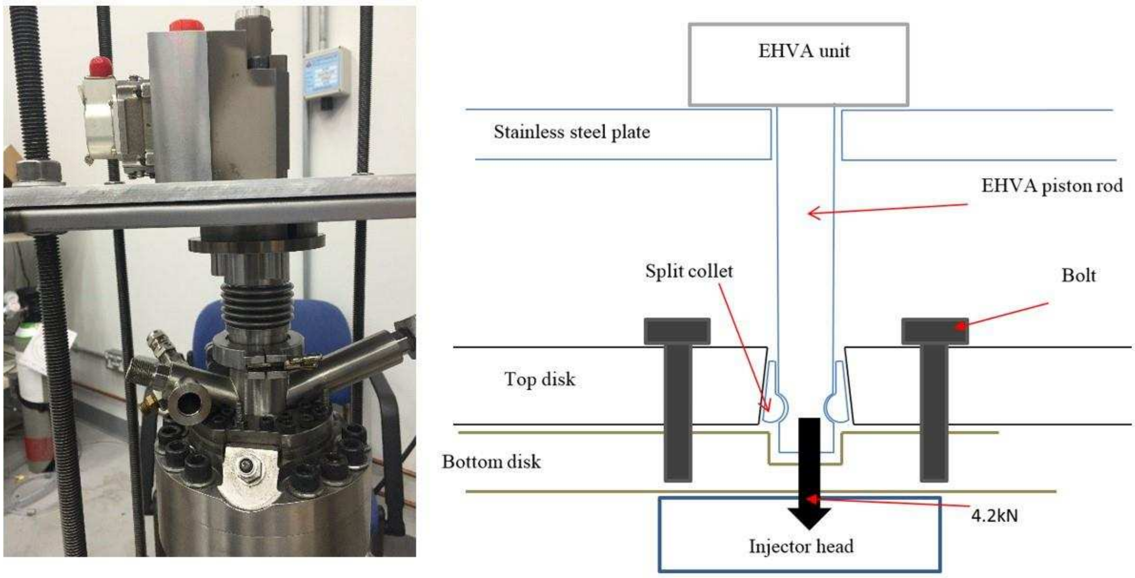

Figure 1: Injector and actuator assembly

2.2 EHVA set up

The EHVA is controlled by a servo valve mechanism. A servo mechanism is a control system that uses its own measured output to accurately match the demand signal. The mechanism minimises the effect of errors or anomalies within the control system itself, as well as the load [19]. It also offers greater precision control of the valve position with a rapid response to changes in speed, direction or frequency.

The hydraulic valve responds to the input signal, with the conversion of fluid pressure into the movement of its own piston rod. This then applies a large axial force onto the head of the injector, which is transmitted to the poppet valve. As a result, the poppet is pushed down to allow the cryogen to flow into the vessel. This is known as the forward stroke. The large force is needed to allow the valve to move independent of any pressure or forces upstream or downstream of it, during both the forward and return strokes. For the forward stroke, the 4.2kN force has to overcome the spring forces and the pressurised LN_2 in the feedline. During the return stroke, the pressure rises in the vessel and the spring forces are most likely to force the valve to close a lot quicker than desired. Therefore the force provided by the EHVA provides better control over the closing of the valve despite the opposing forces.

The hydraulic pressure in the valve actuator is controlled by a unit (Figure 2) consisting of an electrical motor, 5 l/min speed pump, 30 litre oil tank, 2 litre

Figure 2: Hydraulic unit controlling the hydraulic pressure of the EHVA: 1. 50 Hz motor 2. Accumulator 3. Pressure gauge 4. 30 L Oil tank 5. Solenoid by-pass valve 6.

accumulator and a bypass damper for safety. A temperature gauge is incorporated to monitor the oil temperature. This is due to the high fluid temperature caused by constant pumping that could result in failure. The unit has a maximum operating oil pressure of 275 bar which can be used to vary the hydraulic force applied. (Insert Figure 2)

The position of the piston rod of the actuator is measured by a differential variable reluctance transducer (DVRT), with an accuracy of ±2.7 %. The readings are fed to the Data Acquisition system and recorded by the computer running LabVIEW software. The 14-bit Data Acquisition device provides a voltage resolution of 10^{-2} mV per bit and based on the DVRT calibration, the valve lift could be adjusted to the nearest micrometer (10^{-3} mm).

2.3 Control configuration of the EHVA

The servo valve requires a well-designed control system, in order to promptly and accurately open and close the valve in response to the demand signal. Figure 3 shows the components of the closed-loop control system used here. The feedback from the transducer is compared to the demand. The resulting error is amplified and fed back as the new input. The gain of the amplifier is set as high as possible, in order to improve the response and accuracy of the servo valve. This strategy makes the precision of the valve solely dependant on the accuracy of the transducer itself. The output from the DVRT is also amplified by a signal conditioner before the deviation from the demand is calculated. This configuration is used to determine the exact closing time, unlike the previous work[3], where the valve closure was reliant on the valve springs and the pressure gradient.

The injection duration and valve lift were controlled by the width of the demand pulse, which is set manually within the LabVIEW programme. When triggered, the oil in the actuator moves in proportion to the drive signal, resulting in the movement of the piston rod to the desired position. The best valve response was attained using a square wave demand signal of 0 - 1 V, from fully closed to fully opened. The maximum valve lift was recorded at 1.222 mm. (Insert Figure 3)

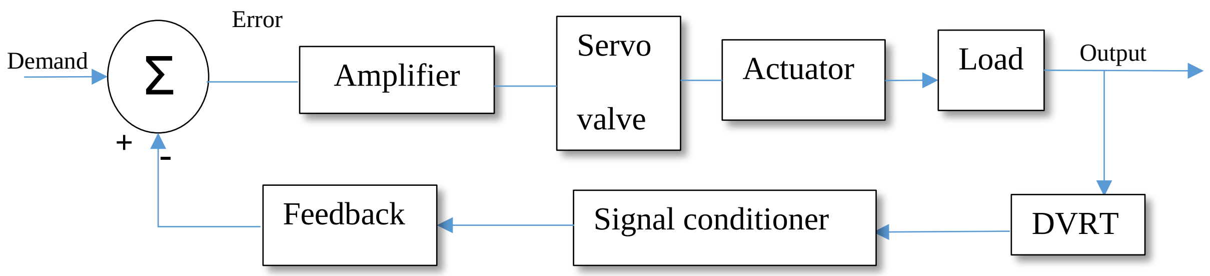

Figure 3: Components in the EHVA servo control mechanism

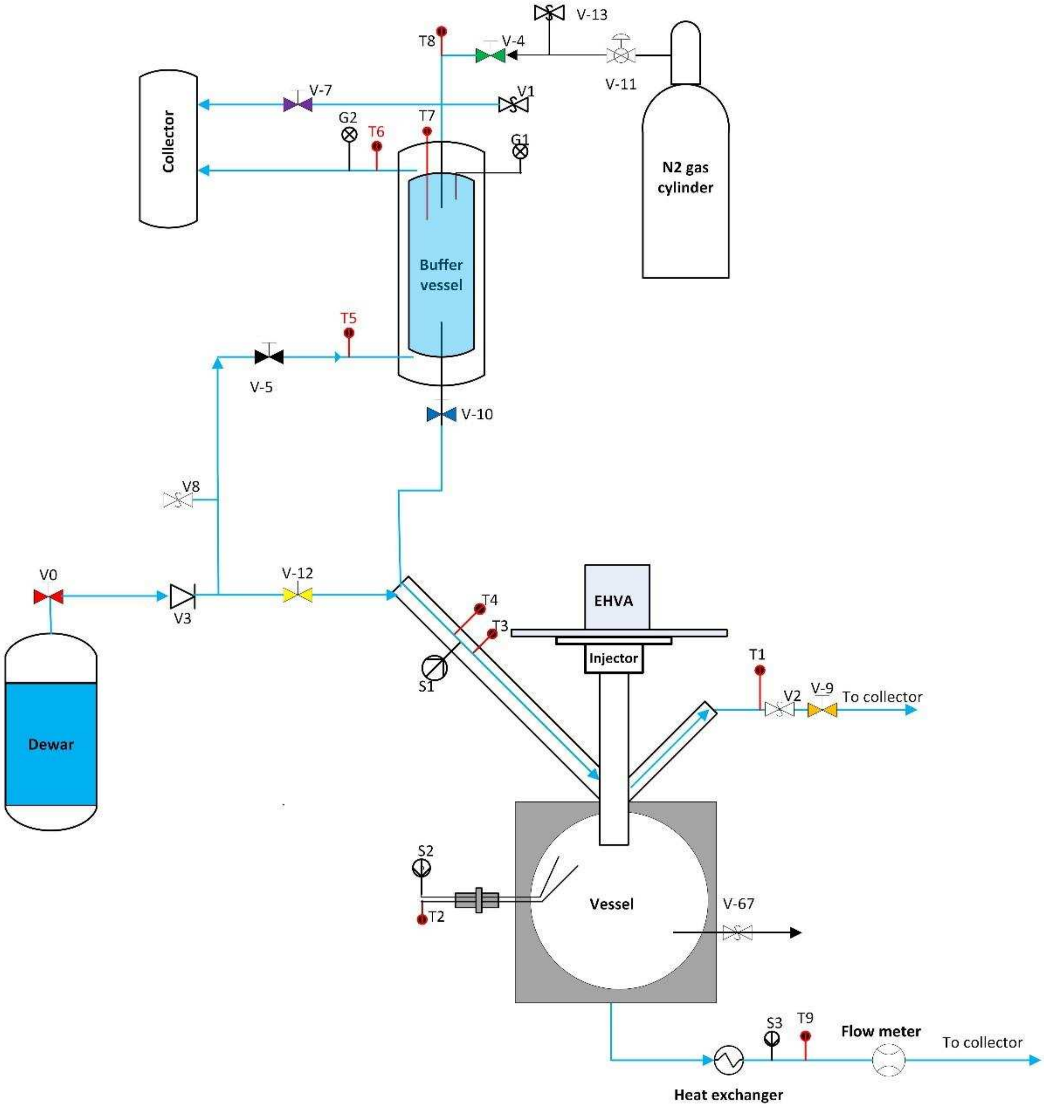

Figure 4: Schematic of the experimental rig in an open configuration

2.4 Experimental setup

The experimental rig (Figure 4 & 5) consists the injector, pressure vessel (pressure bomb), buffer vessel, an EHVA and a data acquisition unit. The primary supply of LN_2 is provided by a 200 L Dewar, which is used to purge the entire system before testing. A manual valve (V5) allows for LN_2 to be delivered to the cooling jacket of the buffer vessel to commence sub-cooling. Sub-cooling occurs continuously throughout testing. The buffer vessel is filled with nitrogen from the Dewar via a vacuum insulated hose and valve V10. Thermocouples T8 and T7 are used to determine when the vessel is filled. Using V4, the LN_2 in the buffer is pressurised using the gas bottle. The pressurised LN_2 has a higher saturation temperature, therefore minimising the occurrence of a multiphase injection, whose thermodynamic properties would be problematic to determine without knowledge of the liquid to vapour ratio in the mixture. The injected LN_2 is vaporised and measured by the flow meter located at the end of the heat exchanger. The measurement uncertainty of the injected mass is mainly due to that of the flow meter of ± 5%.

To achieve consistent and repeatable data, the pressure and temperature of the LN_2 were constantly monitored using several thermocouples and pressure sensors at various locations. The valve was triggered once steady state temperature and pressure readings at the injector were achieved. The pressure was measured by a piezo-resistive transducer (Kulite CT-375) with an uncertainty of ± 5%, whilst temperature readings were recorded by T-type thermocouples, calibrated with a ± 1 % of uncertainty. Thermocouples T1, T3, and T4 were used to monitor the liquid temperature in the injector in order to establish steady flow, and provide information on the heat leak in the

Figure 5: Picture of the assembled experimental rig.

feed line, pre-injection. (Insert Figure 4 & 5)

3. Results

To demonstrate the feasibility of the setup, injections were conducted at various frequencies, pressure, valve lifts, injection durations and sub-cooling ratios (T_{inj}/T_{sat}) of nitrogen; where T_{inj} is the injection temperature and T_{sat} is the saturation temperature at the injection pressure. The parameters of a sample of the tests conducted are shown in Table 1. Control of injection parameters reduces the variables in the injections, thus making the results comparable and repeatable. The flow rate was used to calculate the mass of liquid nitrogen injected. The liquid density was calculated using the reference equation established by Span et al.[20], with an uncertainty of 0.02% for pressures below 300 bar.

Table 1: Sample of some of the injections conducted below saturation temperature and at high pressure, showing the total injected mass and flow rate per injection (per pulse).

Test	Valve lift (h) (mm)	Test duration (s)	Demand Pulse width (ms)	Frequency (Hz)	Injection Pressure (bar)	Temperature T3 (K)	Sub-cooling ratio T_{inj}/T_{sat}	Total LN_2 mass (kg)	Flow rate ($\dot{m}$) kg/s
1	0.51	5.80	5	5	14.58	104.52	0.95	6.02	0.064
2	0.57	4.43	7	5	26.55	102.42	0.84	3.77	0.079
3	1.13	4.63	10	5	28.85	96.82	0.79	3.81	0.084
4	0.55	4.43	7.5	5	29.37	106.78	0.86	3.34	0.081
5	0.59	5.23	7.5	5	44.46	100.41	0.80	3.06	0.097
6	1.18	6.64	10	5	43.54	95.49	0.76	4.18	0.104
7	1.17	4.63	10	5	45.25	96.44	0.77	3.14	0.095

8	0.50	6.03	5	5	46.29	96.89	0.77	3.18	0.095
9	0.61	4.83	7.5	5	47.35	100.46	0.80	2.79	0.098
10	0.51	4.43	5	5	66.34	102.51	0.81	1.74	0.091
11	1.20	5.00	10	5	62.84	108.64	0.78	2.52	0.118
12	1.220	5.00	10	5	71.70	99.40	0.79	2.28	0.115
13	1.16	5.00	10	5	82.22	106.11	0.84	2.13	0.091
14	1.16	5.00	10	2	94.03	110.95	0.88	0.97	0.045

3.1 Valve frequency and lift profiles

Pulsed injections of up to 20 Hz were achieved using the EHVA unit as shown in Figure 6. Frequencies above this were found to cause misalignment of the EHVA piston, due to the increased mechanical vibration in the components. Regardless of the 20 Hz maximum operating frequency, the system can never the less be used to conduct injections corresponding to various engine speeds of up to 1200 rpm, and determine the total injected mass at various injection parameters. With sufficient experimental data, correlations can be established to predict the engine peak pressure and ultimately power output. (Insert Figure 6)

Details of the valve profile are demonstrated in Figure 7.The amplifier provides the signal required for the valve to move to the correct position in respect to the demand. A 4.8 ms delay between the demand and actual valve movement was observed. This delay could be caused by limitations of the hydraulics or the mechanical components of the actuator. That is, it may take slightly longer to redistribute the oil in the valve once it is triggered. It should be noted that the delay was found to vary with the frequency and demand width, however, this was ignored because the valve is still opened and closed within the time specified in the demand. (Insert Figure 7&8)

The valve may only be opened briefly to avoid the onset of backflow in the injector inlet, which would occur as the cylinder pressure rises above that in the feed line. The speed of the valve is controlled by the width of the demand pulse as demonstrated in Figure 8.

The width also determines the height of the valve lift because the valve is given more time to reach its maximum position with a longer pulse. Demonstrated by the 3ms demand, the valve does not have enough time to move to its commanded position before returning to close. To attain the maximum lift, the demand has to be ≥ 10 ms. For a longer pulse, the valve stays open at its maximum lift for longer before commencing the return stroke.

With this in mind, the valve lift and injection timing can be perfected in accordance

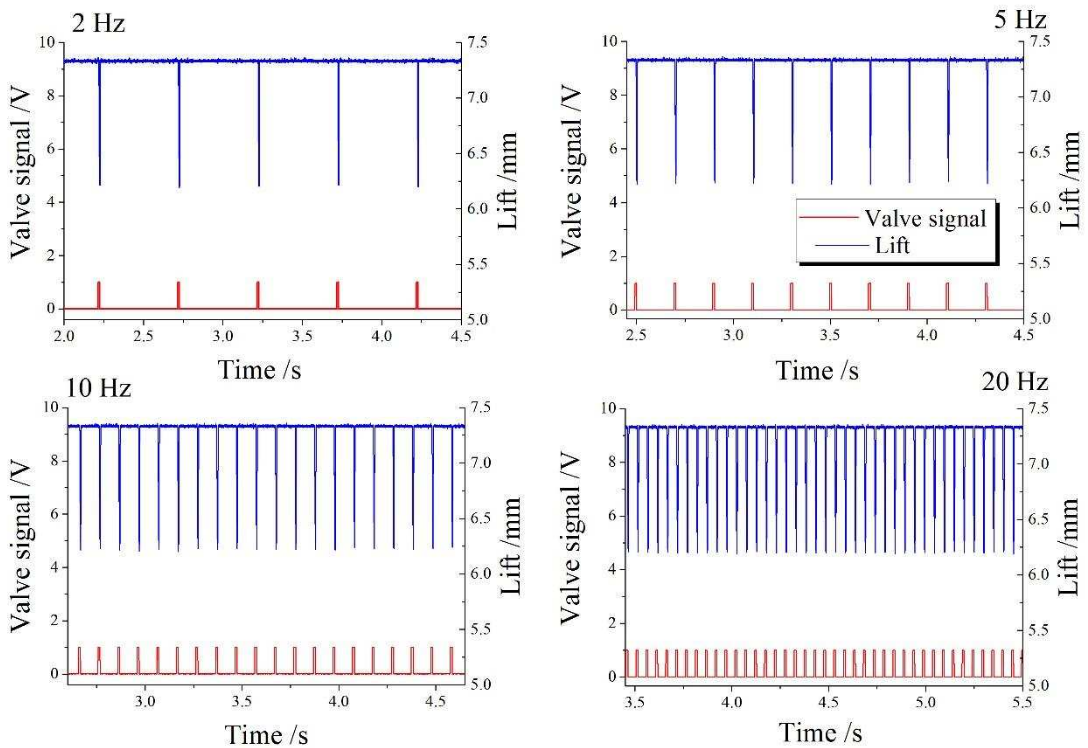

with the engine requirements such as; engine speed, performance or fuel (cryogen) consumption.

Figure 6: Valve profiles of 2,5,10 and 20 Hz frequencies

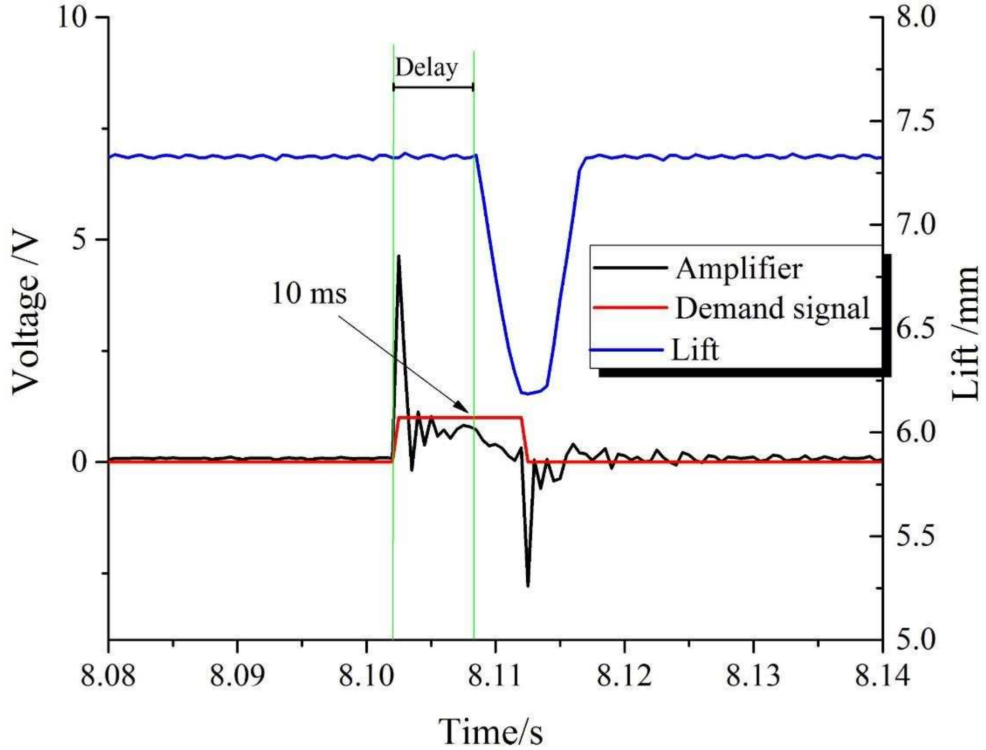

Figure 7: Detail of valve lift profile of a 10 ms demand pulse.

235

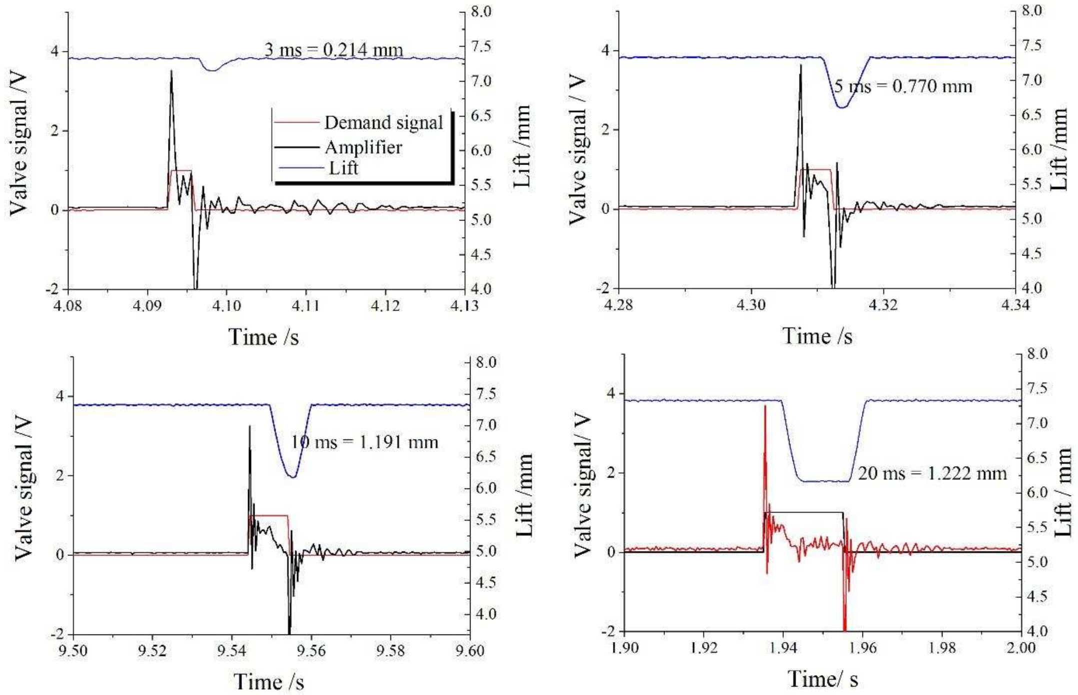

Figure 8: Increase in valve lift with an extended demand period, with maximum lift attained at 10 ms

Pressure drop

When the valve is opened, there is an immediate pressure drop in the upstream pressure in the cryo feed line due to the pressure gradient across the injector as shown

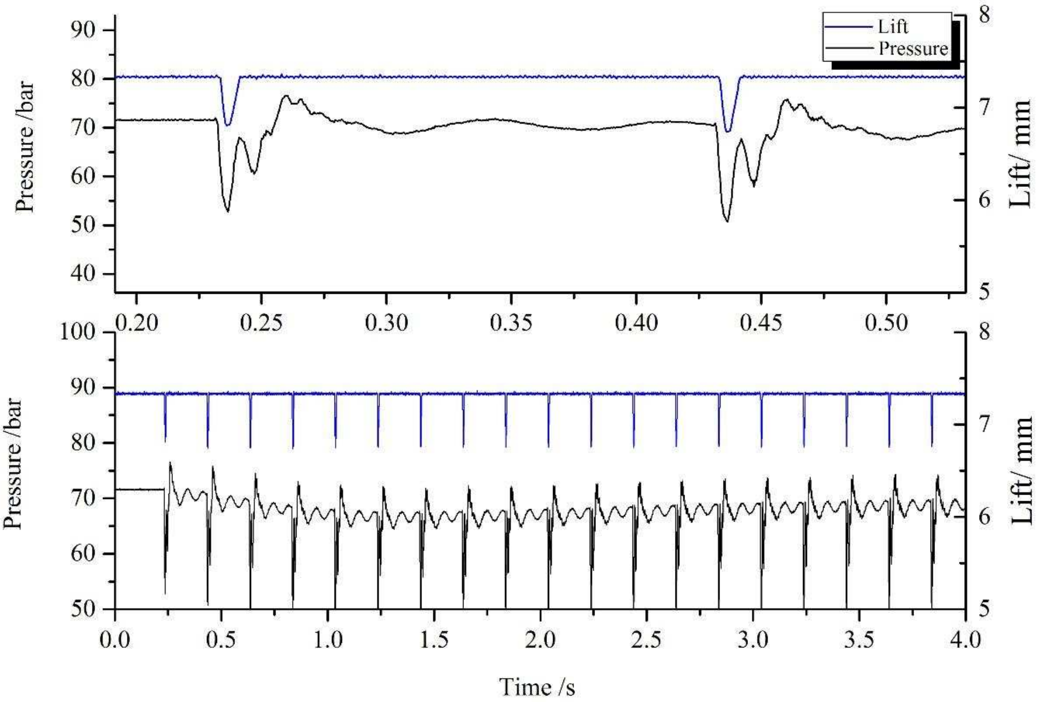

Figure 9: Pressure drop of 18 ±0.05 bar at each pulse and (b) Pressure variation of ±2 bar throughout the entire injection cycle.

Figure 9. A momentary pressure drop of ~18 bar is recorded during each pulse. During the injection cycle, the average pressure remains relatively steady, with a slight variation of $\pm$ 2.2 bar. An increased variation in pressure during the injection would

lead to cyclic variation in the peak cylinder pressure. This can be likened to the jerking in the conventional engine during acceleration, due to the uneven engine power. With a less than 4% variation demonstrated in these tests, jerking was not a concern. The injected mass of a single injection can be scaled up to determine that of pulsed/transient injections, for the same conditions, especially the upstream and downstream pressure ratio. For future work, the pressure variation can be lessened with the use of an accumulator volume of some kind, so as to conduct injections without the significant pressure drop in the upstream. (Insert Figure 9)

3.2 Effects of pressure and cooling ratio on the flow profile

The mass flow profiles obtained for injections at 29, 67, 81 and 83 bar are shown in Figure 10(b). The measured flow was limited by the minimum value recorded by the flow meter at 25 l/s (0.032 kg/s) evident in the cut off points in the graphs below. Above this, the flow increases gradually as its attempts to achieve quasi-steady flow. At this point, the injected nitrogen begins to boil off at the same rate at which it goes through the flow meter. A maximum flow is recorded at the point when the injection is stopped and the flow decreases gradually due to some residual boil off of what is left downstream of the vessel. A comparison of flow profiles for gas and liquid injections at 64 bar is shown in Figure 10(a). (Insert Figure 10)

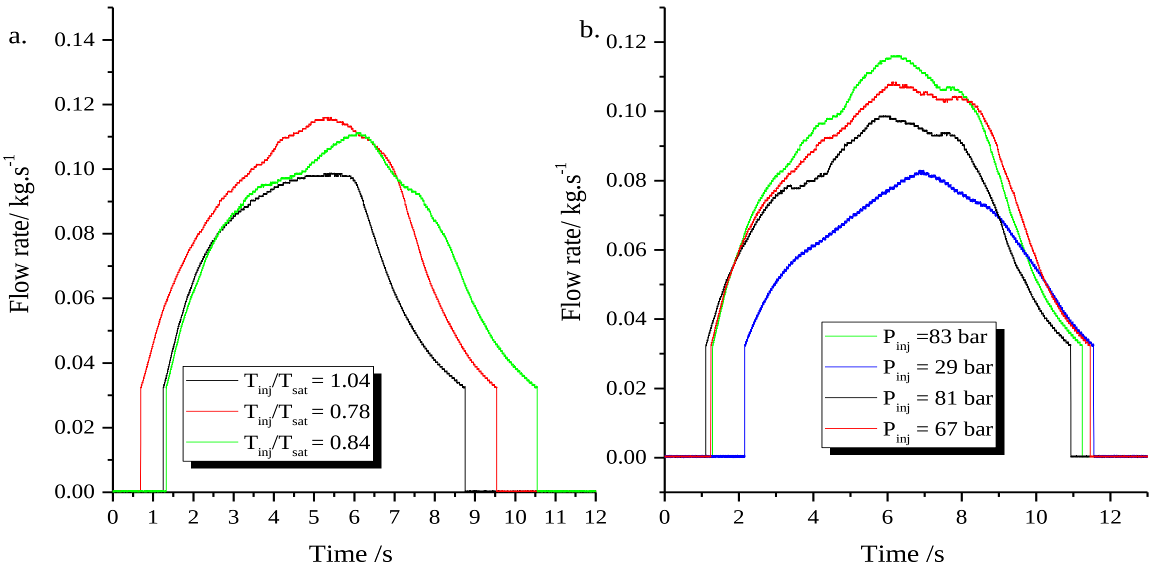

Figure 10: Increase in flow rate with (a) decreased injection temperature and (b) increased injection pressure

The gaseous injection (at a cooling ratio of 1.04) is different because the injected mass is reduced due to a lower fluid density. This is reflected by the lower maximum flow reading of 0.095 kg/s, 1.2 times less than that of the liquid injection at a cooling ratio of 0.78. The initial flow gradient is significantly reduced and the flow plateau's out, indicative of attaining a steady state a lot quicker. With the lack of phase change, the equilibrium temperature is achieved a lot sooner. The higher flow rate in the liquid injections is sustained by the higher energy transfer (latent heat), which continues to increase steadily until the injection is terminated.

The data does not reveal any information on the mass flow profile during the first seconds of the injection, therefore the effects of flashing on the flow were not recorded here. This is due to the minimum measurement of the flow meter at 25 l/s. Flashing is a phenomenon that driven by the temperature and pressure upstream and the pressure downstream of the valve. It is the formation of a gaseous phase in the jet flow due to the rapid pressure drop as the liquid emerges. In theory, this would decrease the mass flow across the valve initially until the liquid begins to flow out. At lower injection temperatures, we would expect a reduction in flashing, resulting in a larger ratio of liquid to gas. However, it is not possible to observe these effects in these experiments. A gradual opening of the valve over a longer time interval, or injection into a pressurised vessel, would reduce the occurrence of flashing due to the reduced pressure drop across the valve. This would facilitate higher pressurisation rates in the engine

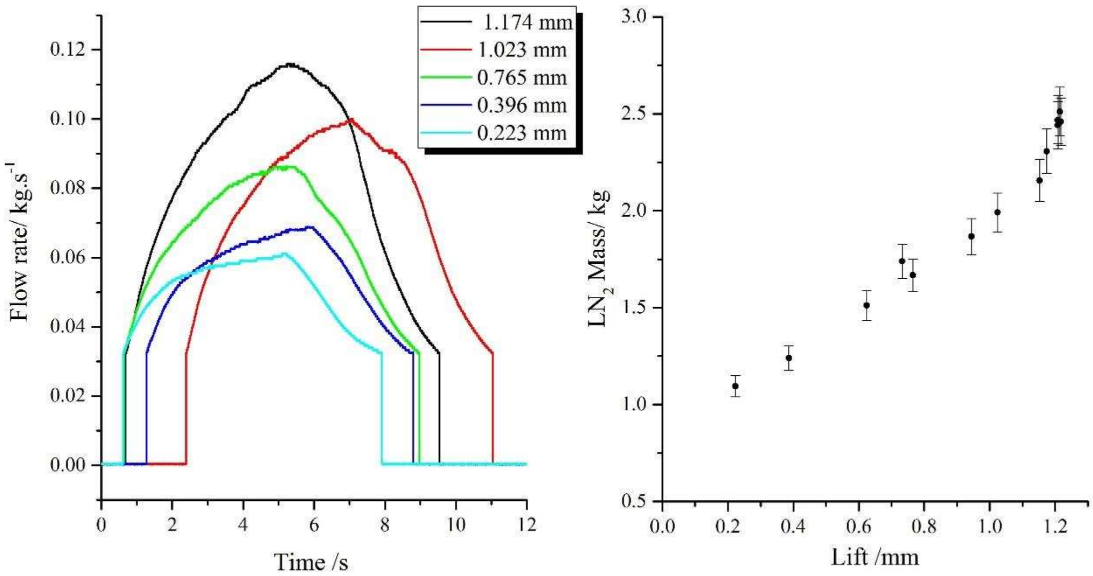

Figure 11: Increase in flow profile with increased valve lift and increased injected mass for injections of 68±1 bar at cooling ratio of 0.84 ± 0.1

cylinder. (Insert Figure 11)

Based on the Bernoulli equation[21], at constant density, flow velocity increases with pressure. However, the flow across the valve is most likely to be critical based on the ratio of the upstream and downstream pressure. For a gas, the flow is choked when the ratio of the downstream to the upstream pressure is less than 0.53. Choked flow is useful because the velocity at the valve is maximised despite variations in the upstream or downstream pressure. With injections into an open vessel, the possibility of choked flow of some description (two-phase choked flow) is high. Under chocked conditions, the flow attains a maximum velocity despite the increase in upstream pressure. However, the mass flow rate increases due to the increased flow density with increased injection pressure.

3.3 Effect of valve lift

The valve lift is proportional to the flow area which is proportional to the mass flow rate, $\dot{m}$. Proof of Equation 1 is evident in the results shown in Figure 11 where A = h * circumference and h = lift.

$$\dot{m} = \rho v A \qquad \text{Equation 1}$$

where ρ is the flow density, v is the flow velocity and A is the flow area.

A 0.2 mm difference in the lift resulted in a 10 kg/s decrease in the flow. Results showed a linear increase in the injected mass with the increased valve lift, due to the increased lift. This correlation can be used to determine the injected mass for a specified lift under these injection parameters, for this valve geometry.

The power and efficiency of the engine are most important. While the power is dependent on the pressurisation, the efficiency is dependent on the speed of the heat transfer process and ensuring the nitrogen is expelled at atmospheric temperature. The mass profile during the injection provides an insight into the heat transfer and ultimately the pressurisation in the cylinder.

4. Conclusions

Direct injection in a cryogenic engine requires a combination of a high mass transfer with a swift injection duration. This paper presents a cryogen injecting system set up and commissioned to allow for the investigations of controlled direct injection for cryogenic engines. The set up consists of a liquid nitrogen supply and a powerful valve actuation system. Designed to conduct several single and steady flow injections of nitrogen in various thermodynamic states, controlled high pressure injections into an open vessel were conducted and studied. The following conclusions can be drawn:

- With the addition of a sub-cooling system, the injection system is capable of performing liquid nitrogen injections at high pressure of up to 94 bar. These tests can be used as a stepping stone into investigations into a closed vessel.

- The use of the EHVA provides accurate control of the valve movement, thus reducing the number of variables in the processes resulting in repeatable and reliable injection data.
- The flow in the system is characterised by the extent of the boil off and attainment of steady flow through the flow meter. This was used to distinguish between liquid and gas injections, highlighting the benefits of latent heat transfer.
- The total injected mass of nitrogen increases with increased injection pressure and valve lift. A definite linear correlation between the lift and injected mass is observed, but there is still no clear trend for the increase in injection pressure.
- The mass flow profiles can be used to calculate the heat transfer to the nitrogen during the injection and provide a better understanding of the pressurisation and how it varies with the injection pressure.

The set up commissioned here can be utilised for further off engine testing such as, the variation of the duration sweep of injections to better identify the transiency of mass flow in an injection event, investigating the heat transfer that results in pressurisation for closed vessel injections, as well as a comparison for future valve design iterations.

Acknowledgements

We are grateful to the financial support from EPSRC, the University of Leeds 110 Anniversary Research Scholarship and Dearman Engine Company Limited. We are also grateful to Paul Edwards (Advanced Engineering Ltd) and Robert Harris (University of Leeds) for all technical support.

5. References

1. Li Y, Chen H and Ding Y. Fundamentals and applications of cryogen as a thermal energy carrier: A critical assessment. *International Journal of Thermal Sciences*. 2010; 49: 941-9.
2. Ltd DEC. Improved cryogenic engine system In: Organisation WIP, (ed.). *World Intellectual Property Organisation*. 10/2016.
3. Clarke H, Martinez-Herasme A, Crookes R and Wen DS. Experimental study of jet structure and pressurisation upon liquid nitrogen injection into water. *International Journal of Multiphase Flow*. 2010; 36: 940-9.
4. Kim T, Kim Y and Kim S-K. Numerical study of cryogenic liquid nitrogen jets at supercritical pressures. *The Journal of Supercritical Fluids*. 2011; 56: 152-63.
5. Branam R and Mayer W. Characterization of cryogenic injection at Supercritical pressure. *Journal of Propulsion and Power*. 2003; 19: 342-55.
6. Mayer W, Telaar J, Branam R, Schneider G and Hussong J. Raman measurements of cryogenic injection at supercritical pressure. *Heat and Mass Transfer*. 2003; 39: 709-19.
7. Mayer WOH, Schik AHA, Vielle B, et al. Atomization and breakup of cryogenic propellants under high-pressure subcritical and supercritical conditions. *Journal of Propulsion and Power*. 1998; 14: 835-42.
8. Archakositt U, Nilsuwankosit S and Sumitra T. Effect of volumetric ratio and injection pressure on water-liquid nitrogen interaction. *Journal of Nuclear Science and Technology*. 2004; 41: 432-9.
9. Wen D, Ding Y and Lin G. Phase change heat transfer of liquid nitrogen upon injection into aqueous based TiO(2) nanofluids. *Journal of Nanoparticle Research*. 2008; 10: 987-96.
10. Wen DS, Chen HS, Ding YL and Dearman P. Liquid nitrogen injection into water: Pressure build-up and heat transfer. *Cryogenics*. 2006; 46: 740-8.
11. Dinh TN, Bui VA, Nourgaliev RR, Green JA and Sehgal BR. Experimental and analytical studies of melt jet-coolant interactions: a synthesis. *Nuclear Engineering and Design*. 1999; 189: 299-327.
12. Dahlsveen J, Kristoffersen R and Saetran LR. Jet mixing of cryogen and water. *TSFP DIGITAL LIBRARY ONLINE*. Begel House Inc., 2001.
13. Maytal B-Z and Elias E. Two-phase choking conditions of real gases flow at their critical stagnation temperatures and closely above. *Cryogenics*. 2009; 49: 469-81.
14. Mohr S, Clarke H, Garner CP, Rebelo N, Williams AM and Zhao HY. On the Measurement and Modeling of High-Pressure Flows in Poppet Valves Under Steady-State and Transient Conditions. *Journal of Fluids Engineering-Transactions of the Asme*. 2017; 139.
15. Hambir S and Jog JP. Sintering of ultra high molecular weight polyethylene. *Bulletin of Materials Science*. 2000; 23: 221-6.

16. Wang A, Essner A, Polineni VK, Stark C and Dumbleton JH. Lubrication and wear of ultra-high molecular weight polyethylene in total joint replacements. *Tribology International*. 1998; 31: 17-33.
17. Sudo M and Muraki T. Sealing stopper for a syringe and a prefilled syringe. Google Patents, 2000.
18. Liu HT, Ji HM and Wang XM. Tribological properties of ultra-high molecular weight polyethylene at ultra-low temperature. *Cryogenics*. 2013; 58: 1-4.
19. Rydberg K-E. Hydraulic servo systems. *TMHP51 Fluid and Mechanical Engineering Systems Linköping University*. 2008.
20. Span R, Lemmon EW, Jacobsen RT, Wagner W and Yokozeki A. A reference equation of state for the thermodynamic properties of nitrogen for temperatures from 63.151 to 1000 K and pressures to 2200 MPa. *Journal of Physical and Chemical Reference Data*. 2000; 29: 1361-433.
21. Shames IH and Shames IH. *Mechanics of fluids*. McGraw-Hill New York, 1982.